Article ID: 1007-4627(2016) 03-0330-06

Comparison Study between ADS Granular and Monolith Targets Using Monte Carlo Method

CHEN Jianqi[1,2], ZHANG Yaling[1], ZHANG Xunchao[1], YAN Xuesong[1],
LI Jianyang[1], YANG Lei[1]

(*1. Institute of Modern Physics, Chinese Academy of Sciences, Lanzhou 730000, China*;
2. University of Chinese Academy of Sciences, Beijing 100049, China)

Abstract: Using the Fluka Monte Carlo code, the comparison study between granular target and monolith target in neutron and proton leakages, neutron and proton fluxes, energy deposition density and residual radioactivity as well as gamma dose rates were presented. Results shows that the neutron flux and energy deposition in tungsten spheres target are more homogeneous along the axial direction than monolith target. What's more, the granular target has a more lateral neutron yield and a relatively small amount of neutrons in the backward direction. In addition, the total radioactivity is found to be comparatively lower in granular target, although for some nuclei, the value of their activities are similar for both targets. So the above features make the granular target more suitable as a ADS target.

Key words: ADS; spallation target; granular target; monolith target; activity; particle transport simulation; residual gamma dose rate

CLC number: O532.33 **Document code:** A **DOI:** 10.11804/NuclPhysRev.33.03.330

1 Introduction

High power beam of protons has applications in the production of high intensity secondary beams of neutrons, muons, kaons and neutrinos as well as in nuclear waste transmutation and accelerator-driven system (ADS)[1]. Transmutation of nuclear waste in ADS system typically requires 350 MeV $\sim$ 1 GeV accelerators delivering proton flux of $5 \sim 10$ mA for demonstrators, and $20 \sim 50$ mA for larger industrial systems[2]. Thus it means that higher power (>1 MW) targets are required to be built for ADS of exceptional reliability.

Although there is only a relatively small number of spallation neutron sources currently in operation world wide, substantial efforts are being made to develop target systems that can serve in a new generation of facilities whose proton beam power is of several megawatts[3]. Major concern with solid target is the ability to cool at proton beam power above 1 MW[4], considering about 50% of beam energy is deposited in the target. A few alternative target systems are under consideration, like rotating solid target[5], flowing liquid metal target[6], plate target[7], rod target[8], segmented target and granular target. Using a rotating solid target is an option in certain cases but still has to cope with the instantaneous load levels[3]. Liquid target like mercury target has been operated in SNS under 1.4 MW irradiation, although liquid target has the difficulty in cavitation, corrosion and splashing[9–10]. A stationary granular target has been proposed by Seviers to solve this problem used for neutrino factory[11–12] and the test experiment of the granular target has been made in High Radiation to Materials facility (HiRadMat) at CERN[13]. This target configuration was also proposed to be used in beam dump[14] and neutron source[15].

In summary, the advantages of the packed-bed target are as follows: (a) large surface area for heat transfer with coolant, which is able to access areas with highest energy deposition; (b) minimal thermo-mechanical and inertial stresses; (c) potential heat removal rates at the hundreds kilowatt level with high helium flow rate[16].

A mercury target and a stationary target made up of tantalum pellets, irradiated by a 2.2 GeV, 4 MW proton beam, are compared from a radiological

Received date: 18 Oct. 2015; **Revised date:** 10 Nov. 2015

Foundation item: Strategic Priority Research Program of Chinese Academy of Sciences (XDA03030100); National Natural Science Foundation of China(91026005)

Biography: CHEN Jianqi(1989–), male, Guyuan, Ningxia, postgraduate, working on the particle physics and nuclear physics;

Corresponding author: YANG Lei, E-mail: lyang@impcas.ac.cn.

point of view by Agosteo[17]. While the monolith target and the granular target have never been compared before, so in the present work, we compared the monolith tungsten target with a stationary target filled with the tungsten spheres and helium under the irradiation of 1 GeV, 1 mA proton beam from the same point of view. An estimation of proton flux, neutron flux, power density and induced activity was also performed for both targets. Furthermore, the major nuclei contributing large amounts of total activity were listed and the reason leading to the discrepancy of activity in two targets was also analyzed.

2 The granular target and the monolith target

The granular target was approximated as an homogeneous cylinder (55 cm length, 15 cm radius) made of tungsten with an effective density of 11.165 g/cm^3. In addition, a 0.5 cm thick layer of 316L stainless steel (Fe 75%, Ni 12%, Cr 8%, Mo 2%, Mn 2% and Si 1%) was used to enclose the small tungsten spheres. There are about 43 067 pellets of a 5 mm diameter with a total weight of 433 844 g cooled by helium under standard atmospheric pressure.

The monolith target had the same dimensions but with a natural tungsten's density (19.25 g/cm^3). The projected range in tungsten is 31 cm under incident protons of 1 GeV. While considering the lower stopping power in the granular target, the length here was set as 55 cm. Sectional views of the modeled geometry are shown in Fig. 1.

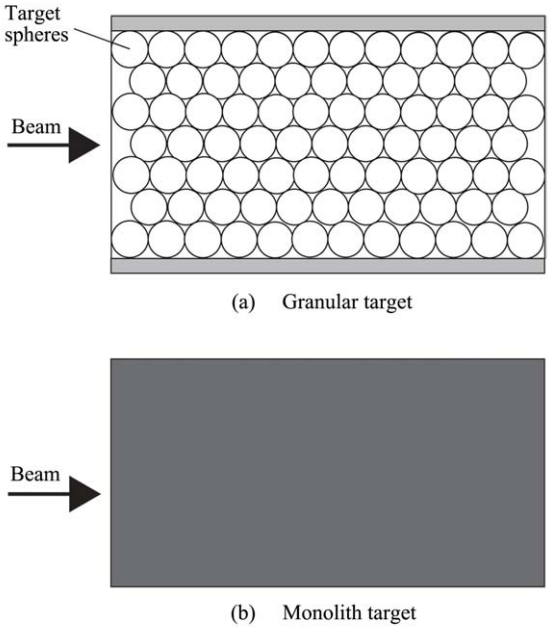

Fig. 1 Schemes of Granular target and Monolith target.

3 Monte Carlo simulation

The Monte Carlo cascade code FLUKA[18–19] was used here to estimate proton flux, neutron flux, power density and induced activity expected in two targets. The source term has been defined as a 1 GeV proton beam of an annular profile ($r = 3.0$ cm), without the momentum spread of divergence. A total of 1 000 000 primary histories were simulated in every run.

First of all, the IRRPROF card was used to set up a time profile of irradiation with 1 mA beam current after one month of operation, then 12 cooling times; 0 s, 1, 10 h, 1, 2, 10, 30 d, 6 months, 1, 2, 5 and 10 a after the beam shutdown were defined by the DCYTIME card. The induced activity was then estimated by using the RESNUCLE card while the residual gamma dose rates were estimated at the same cooling times by using the USRBIN cards, following with the AUXSCORE card to obtain the ambient dose equivalent at surfaces. Afterwards, the spatial distributions of neutron flux, proton flux and power density were all recorded by USRBIN card. Finally, the mechanisms of coalescence and evaporation involved in the reaction were then correspondingly activated by COALESCE and ECAPORAT in the PHYSICS cards.

4 Results and discussion

4.1 Neutron yield and neutron flux

Just as expected by the theory[20], radially, the neutron (proton, power density) distribution is determined essentially by the intensity profile of the incoming beam (3 cm radius beam spot here), which widens somewhat as it travels down the length of the target. Axially, after the building up of neutron yield (proton yield, power density) at target head due to intranuclear cascade(INCL), neutron yield decreases exponentially along the axis of the target caused by competing processes such as ionization losses below 100 MeV, pair production and other effects at the high energy end.

The simulated results shown in Fig. 2 fairly agree with the prediction of the theory, and so do the proton flux and power density seen from Figs. 3 and 4. As can be seen in Fig. 2, neutron leakage from the granular target that has lower stopping power is higher than that from the monolith target, especially in the forward direction. The maximum value of neutron flux in later target (2.26×10^{15} n/(s· cm^2· mA) at 5 cm) is higher than that in the granular target (1.09×10^{15} n/(s· cm^2 · mA) at 5.5 cm). This is due to the higher macroscopic cross-section for nuclear interactions in the monolith case that have a higher density. The leakage of neutrons (protons, gammas) from the target boundary is also listed in Table 1, which is in coincidence with the

Fig. 2. Forward leakage of neutrons are negligible in comparison to lateral neutron leakage for both targets, while the backward leaked neutrons account for a significant portion of neutrons. This can be explained as there is a neutron buildup near the front face of the target, neutrons scatter more easily backward than in any other directions. This is a major drawback that the backward neutrons may reach the beam tunnel causing activation problems in the beam line structures[20]. In the backward direction, the granular target produce

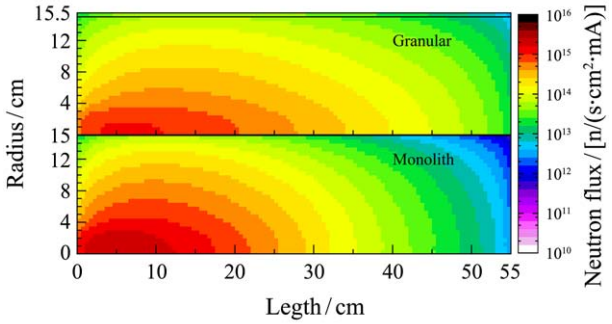

Fig. 2 Contour plots of neutron flux in the granular and monolith targets irradiated by 1 GeV protons. Here we only depict its upper half-space due to the axisymmetric distribution of neutron flux. The following contour plots of proton flux, energy deposition and induced activity are handled in the same way.

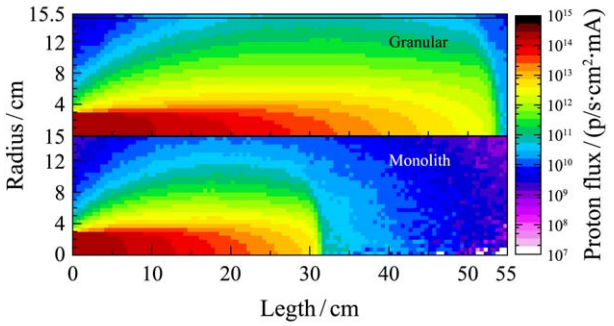

Fig. 3 Proton flux in the granular and monolith targets irradiated by 1 GeV protons.

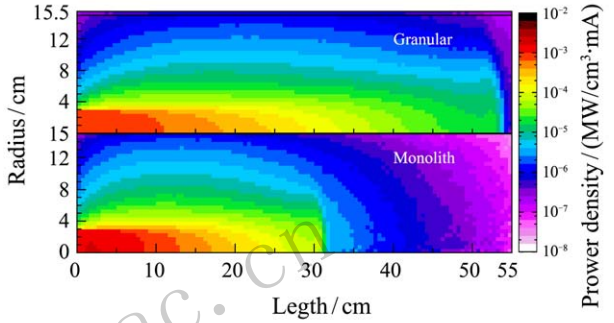

Fig. 4 Energy deposition density (GeV/cm^3) in the granular target and monolith targets irradiated by 1 GeV protons.

less neutrons. So the granular target is more suitable choice for ADS target from this point.

Table 1 The production yields of neutron, proton and photon along the forward, lateral and backward directions for both targets.

Production	Forward		Lateral		Backward		Total	
	Granular	Monolith	Granular	Monolith	Granular	Monolith	Granular	Monolith
Neutron	6.17×10^{-1}	9.04×10^{-2}	1.57×10^{1}	1.22×10^{1}	4.84×10^{0}	7.34×10^{0}	2.12×10^{1}	1.96×10^{1}
Proton	1.28×10^{-3}	1.24×10^{-4}	1.66×10^{-2}	3.49×10^{-3}	8.68×10^{-3}	8.81×10^{-3}	2.65×10^{-2}	1.24×10^{-2}
Photon	4.83×10^{-2}	6.41×10^{-3}	1.33×10^{0}	7.26×10^{1}	8.15×10^{-1}	9.71×10^{-1}	2.19×10^{0}	1.70×10^{0}

4.2 Proton flux and power density

Figs. 3 and 4 show the distributions of proton flux and power density in the granular and monolith targets. Two targets have the similar distribution that the location of maximum is closer to the front surface compared with the neutron flux. For more than 60% of the total energy of the incident 1 GeV proton beam is dissipated in the target. The maximum power density is about 0.000 89 MW/cm^3 per mA (at 2.5 cm) in the granular target while 0.001 6 MW/cm^3 per mA (at 1.5 cm) in the monolith target. Correspondingly, the total energy deposition in the granular case is about 0.68 MW per mA, more than 8% decrease in comparison with the monolith case (0.74 MW per mA). This means that the 8% beam power is carried away by the additionally leaking particles, most of which are neutrons. In fact, it can be also seen in Table 1 that lateral neutron yield for the granular target is greater by about 22%, with respect to the monolith target. What's more, Figs. 2 and 4 indicate that the neutron flux and power density are better homogenized along the length of the granular target, another feature expected by the ADS.

4.3 Induced activity

In Fig. 5, a typical contour plot of residual activity is shown, which is similar with the nuclide chart but no stable nuclei. During the spallation process, not only neutrons but also protons and other light nuclei are emitted. As a result, the residual nuclei are not only neutron-poor isotopes of the parent nucleus that decay into lower Z elements, but these elements created directly in the spallation process and even for

fission products of the medium-heavy and light nuclei from excited nucleus[20]. The light nuclei, medium-heavy nuclei, heavy nuclei created by those processes can also be found in Fig. 5 with different radioactivity. The radionuclide inventory after one month of operation is determined not only by its decay constant but also its generation rate. Therefore it is easy to understand that some nuclei with high decay constant but with low radioactivity as shown in Fig. 5.

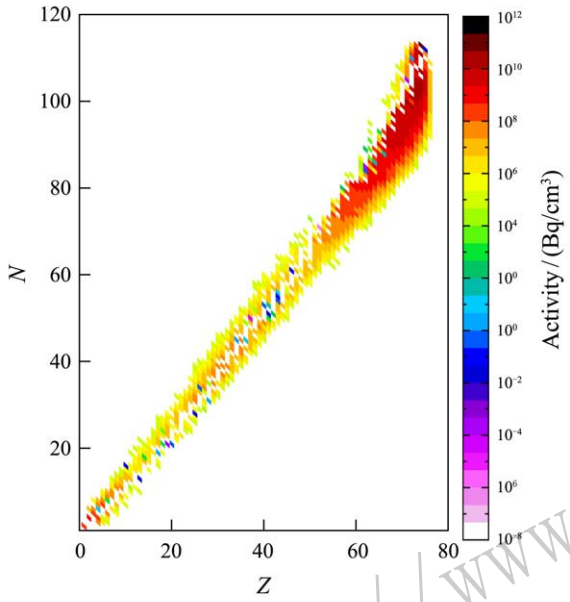

Fig. 5　A contour plot of the residual nuclei formed in the granular target.

The simulated and empirical results of the total activity generated in both targets as a function of decay time are shown in Fig. 6. In addition, the contour plots of residual activity for two targets after one month irradiation are also depicted in Fig. 7. The overall activity comes down by about four orders of magnitude as the cooling time increases from 1 h to 10 a. After ceasing the facility, the total activities, contributed by several nuclides, are about 6.45×10^{16} Bq and 1.07×10^{17} Bq separately for the granular target and monolith target. However, the empirical relation proposed by Sullivan[21] gives a result more by a factor 1, when compared with the simulated result.

The induced activity (S, Bq) in heavy element target after irradiation in a beam of Φ protons per cm^2 per second is

$$S=1.8\times10^{-3}V\rho\Phi\left[t^{-0.4}-(T+t)^{-0.4}\right], \qquad (1)$$

where V and ρ separately refer to volume and density, T and t are irradiation and cooling times respectively in days.

As presented in Fig. 6, the induced activity appears higher in the monolith target at the time of shutdown. This result can be also referred by the leakage of neutrons, protons and photons in Table 1. It is evident that more secondary particles are emitted from granular target. Moreover, the number of inelastic interaction (stars) scored in the granular target is 3.73 595 stars per proton, while 4.47 673 stars in the monolith target. Consequently, it is an advantage for granular target for further reduction in activation and damage problems.

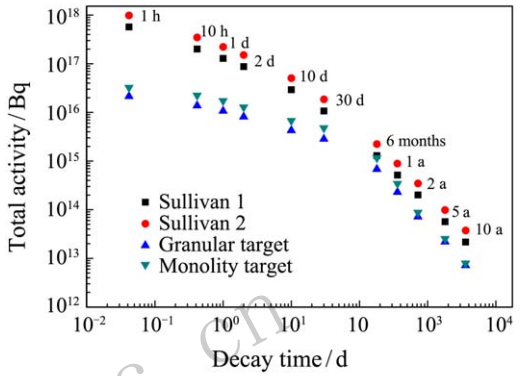

Fig. 6　Induced activity (Bq) in the granular and monolith targets after one month of operation, as a function of cooling time. Also given the results obtained from an empirical relation proposed by Sullivan. The suffix 1 here refers to the granular target, and the suffix 2 to the monolith target.

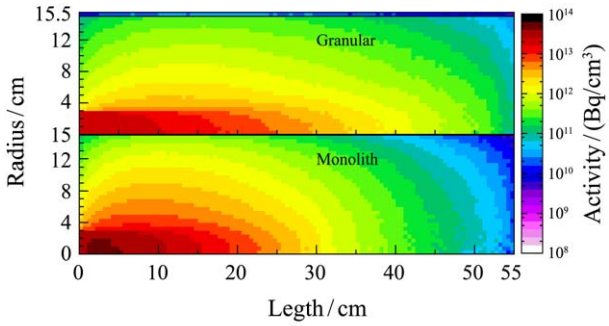

Fig. 7　Induced activity (Bq/cm^3) in the granular and monolith targets irradiated by 1 GeV protons of 1 mA beam current after one month of operation.

The major nuclides in two targets, contributing more than 1% of the total activity, are listed in Table 2. The discrepancy of activity of those nuclides leads to the discrepancy of total activity for two targets. Those produced nuclides are mainly contributed by neutron interactions with energies below 20 MeV[22]. For instance, ^{187}W is produced through the neutron capture reaction of ^{186}W (n,γ) ^{187}W. However, there are some nuclides (listed in Table 3) that they almost have the same value of activity for two targets due to the high energy proton interactions.

The discrepancy of radioactivity between two targets becomes small with the evolution of time as shown in Fig. 6. This variation can be explained that most

of nuclides listed in Table 2 are short-lived (less than 10 days) and decay on a short time scale.

Table 2 The most important radioactive nuclei scored in the granular target and in the monolith target after 30 days of operation. All results have an uncertainty lower than 0.5%.

Residual nuclei		Activity ($\times 10^{10}$ Bq/cm^3)		$\frac{A_m - A_g}{A_m}$
Isotope	Half life	Granular	Monolith	(%)
^{187}W	23.7 h	10.0	27.3	63.2
^{185}W	75.1 d	4.07	9.36	56.5
^{179}W	2230 s	3.65	4.68	22.0
^{178}W	21.6 d	2.00	2.54	21.2
^{177}W	2.20 h	2.03	2.51	19.2
^{176}W	2.50 h	1.76	2.16	18.4
^{178}Ta	2.36 h	2.44	3.08	20.7
^{177}Ta	2.35 d	2.99	3.68	18.7
^{176}Ta	8.09 h	2.53	3.08	17.9
^{175}Ta	10.5 h	1.91	2.25	15.1
Total radioactivity		166	275	39.6

Table 3 The residual nuclei in granular target and monolith targets have the almost equivalent activity after 30 days of irradiation. All results have an uncertainty lower than 5%.

Residual nuclei		Activity ($\times 10^{8}$ Bq/cm^3)		$\frac{A_m - A_g}{A_m}$
Isotope	Half life	Granular	Monolith	(%)
^{172}Re	55.0 s	1.62	1.61	-0.595
^{165}Ta	31.0 s	4.39	4.35	-0.955
^{162}Lu	11.4 s	8.86	8.77	-0.993
^{155}Tm	45.0 s	3.19	3.17	-0.891
^{157}Er	1120 s	22.7	22.7	-0.049
^{153}Ho	558 s	5.58	5.56	-0.306
^{157}Dy	8.14 h	27.0	27.0	-0.093
^{150}Tb	3.48 h	12.7	12.6	-0.643
^{147}Tb	1.70 h	7.82	7.76	-0.724
^{146}Tb	23.0 s	2.12	2.11	-0.722
^{147}Gd	1.59 d	16.6	16.6	-0.380
^{147}Eu	24.1 d	9.70	9.63	-0.784
^{145}Eu	5.93 d	12.0	11.9	-0.653
^{140}Nd	3.37 d	5.60	5.60	-0.114
^{137}Nd	2310 s	2.86	2.85	-0.337
^{140}Pr	203 s	5.64	5.64	-0.114
^{139}Pr	4.41 h	3.28	3.28	-0.049
^{129}Cs	1.34 d	1.12	1.11	-0.440

4.4 Gamma Dose Rates

Fig. 8 shows the gamma ambient dose equivalent rates ($H_\gamma * (10)$) from the front, lateral and back target surfaces. The total ambient dose equivalent rate at surfaces after irradiation of 30 days is 3.56×10^{12} pSv/s for granular target while 3.36×10^{12} pSv/s for monolith target. Photons are emitted either promptly during intranuclear cascade process, or during de-excitation stage of the pre-fragments produced aftermath of spallation reactions. Due to the influence of INCL mechanism, both targets have an anisotropic gamma spectrum distribution. In addition, most of the residual nuclei are concentrated at the beginning of the target. The dose rates here in the backward direction are much larger compared to those in the forward or lateral directions, which also occurs in the LBE target[23]. However, in forward direction, gamma dose rates in the monolith target are reduced by about a factor of 1 when compared with those in the granular target, which is in coincidence with Table 1 and Fig. 8. It should be underlined that both targets have a long distance to the recycling limit[24] after 10 years decaying.

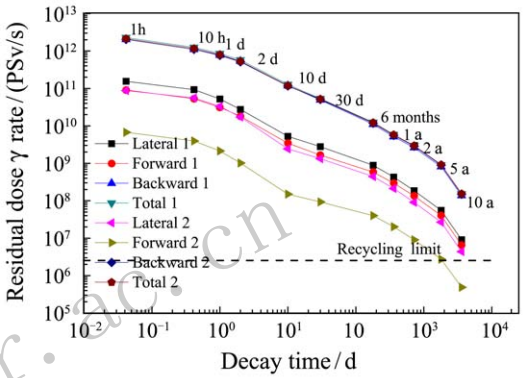

Fig. 8 Residual gamma dose rates (pSv/s) along the lateral, forward and backward directions in the granular (suffix 1) and monolith (suffix 2) targets after one month of operation, as a function of cooling time.

5 Conclusion

The comparison between granular target and monolith target in flux profile, residual activity and gamma dose rates, under irradiation of 1 GeV protons for after one month of irradiation, has been made by using the FLUKA Monte Carlo code. Neutron production is more homogeneous along the axial direction in the case of granular target. What's more, the granular target effectively enhances the lateral neutron yield and decreases the neutrons leaked in the backward direction. In addition, it has a relatively small amount of deposited energy and the special construction make it easier to cool. So the granular target is more suitable to be as a ADS target under MW level irradiation. The total radioactivity in the granular target is lower than that in the monolith target. Although for some radioactive nuclei, their activities in the former case are nearer to those in the later case. Finally, the gamma dose rates for two targets at three directions are also analyzed. Both targets have a long distance to recycling limit and need more decay time.

This is a preliminary study of granular target from the aspects of radiation protection under the MW level. The target considered here is an idealized target that the helium is in a status of static at a pressure of 1

atm but not of a velocity of 100 m/s at 20 atm proposed by Seviers for neutrino factory. Further studies are therefore necessary to consider the effect of helium transverse cooling under high pressure condition.

Acknowledgement Dr. Zhang Sheng and Dr. Zhang Yuezhao from the Institute of Modern Physics, Chinese Academy of Sciences are appreciated for their generous assistance.

References:

[1] ROSER T. Plans for Future Megawatt Facilities[M]. 2005, **773**: 11.
[2] BIARROTTE J L, BOUSSON S, JUNQUERA T, *et al*. Nucl Instr Meth A, 2006, **562**(2): 656.
[3] BAUER G S. J Nucl Mater, 2010, **398**(1): 19.
[4] APOLLONIO M, BERG J S, BLONDEL A, *et al*. JINST, 2009, **4**(07): P07001.
[5] BENNETT J R J. Nucl Instr Meth A, 2000, **451**(1): 344.
[6] ABDERRAHIM H A, AOUST T, MALAMBU E, *et al*. Radiat Prot Dosim, 2005, **116**(1-4): 433.
[7] BROOME T A. High Power Targets for Spallation Sources[C]. 1991, KEK-Report 90-25.
[8] FISCHER W E. Physica B, 1997, **234**: 1202.
[9] HAINES J R, RIEMER B W, FELDE D K, *et al*. J Nucl Mater, 2005, **343**(1): 58.
[10] FUTAKAWA M, NAOE T, TSAI C C, *et al*. J Nucl Mater, 2005, **343**(1): 70.
[11] PUGNAT P, SIEVERS P. J Phys G, 2003, **29**(8): 1797.
[12] SIEVERS P. Nucl Instr Meth A, 2003, **503**(1): 344.
[13] EFTHYMIOPOULOS I, CHARITONIDIS N, CARETTA O, *et al*. XIIIth International Workshop on Neutrino Factories, Super Beams and Beta Beams. 2011 (EPFL-POSTER-170582).
[14] WALZ D R, LUCAS L R. IEEE Transactions on Nuclear Science, 1969, **16**(3): 613.
[15] AMMERMAN C, WOLOSHUN K, HE X, *et al*. ANS Winter Meeting, Los Alamos National Laboratory. 2001.
[16] BAUSSAN E, DRACOS M, GAUDIOT G, *et al*. Journal of Physics: Conference Series. IOP Publishing, 2013, **408**(1): 012061.
[17] AGOSTEO S, MAGISTRIS M, SILARI M. Nucl Instr Meth A, 2005, **545**(3): 813.
[18] FERRARI A, SALA P R, FASSO A, *et al*. FLUKA: A Multi-particle Transport Code (Program Version 2005)[R]. 2005.
[19] BATTISTONI G, CERUTTI F, FASSO A, *et al*. Hadronic Shower Simulation Workshop(AIP Conference Proceedings Volume 896). 2007, **896**: 31.
[20] SHETTY N V. Study of Particle Transport in a High Power Spallation Target for an Accelerator-driven Transmutation System[D]. University Library, 2013.
[21] SULLIVAN A H. A Guide to Radiation and Radioactivity Levels Near High Energy Particle Accelerators[M]. Ashford, Kent, England: Nuclear Technology Publishing, 1992, pp. 103-104.
[22] KONOBEYEV A Y, FISCHER U, ZANINI L. Nucl Instr Meth A, 2009, **605**(3): 224.
[23] SUNIL C, BIJU K, SARKAR P K. Nucl Instr Meth A, 2013, **719**: 29.
[24] SEIDEL K, EICHIN R, FISCHER U, *et al*. Fus Eng Des, 2006, **81**(8): 1211.

应用蒙特卡罗方法对比研究 ADS 颗粒靶和块状靶

陈建琪[1,2]，张雅玲[1]，张勋超[1]，闫雪松[1]，李建洋[1]，杨 磊[1]

(1. 中国科学院近代物理研究所，兰州 730000;
2. 中国科学院大学，北京 100049)

摘要： 应用蒙特卡罗软件FLUKA对比研究了颗粒靶和块状实体靶在中子、质子泄露，中子、质子流强，能量沉积，残余核活度及Gamma射线剂量率的差异。最终结果显示在靶的轴对称方向，相较块状靶，颗粒靶中的中子流强和能量沉积更加均匀，且侧壁泄露中子更多而反冲中子较少。除此之外，在散裂产物放射性方面，尽管有部分核素两种靶具有相似的活度，但是颗粒靶总的放射性活度要比块状靶低。因此以上特性使得颗粒靶相较块状实体靶更适合用于ADS的靶。

关键词： ADS；散裂靶；颗粒靶；块状靶；活度；粒子输运模拟；残余Gamma剂量率

收稿日期： 2015-10-18　**修改日期：** 2015-11-10
基金项目： 中国科学院战略性先导专项(XDA03030100)；国家自然科学基金资助项目(91026005)
通信作者： 杨磊，E-mail：lyang@impcas.ac.cn。